

Nanoscale Morphology of Conjugated Polymer/Fullerene-Based Bulk-Heterojunction Solar Cells**

By Harald Hoppe,* Michael Niggemann, Christoph Winder, Jürgen Kraut, Renate Hiesgen, Andreas Hinsch, Dieter Meissner, and Niyazi Serdar Sariciftci

The relation between the nanoscale morphology and associated device properties in conjugated polymer/fullerene bulk-heterojunction “plastic solar cells” is investigated. We perform complementary measurements on solid-state blends of poly[2-methoxy-5-(3,7-dimethyloctyloxy)]-1,4-phenylenevinylene (MDMO-PPV) and the soluble fullerene C₆₀ derivative 1-(3-methoxycarbonyl) propyl-1-phenyl [6,6]C₆₁ (PCBM), spin-cast from either toluene or chlorobenzene solutions. The characterization of the nanomorphology is carried out via scanning electron microscopy (SEM) and atomic force microscopy (AFM), while solar-cell devices were characterized by means of current–voltage (*I*–*V*) and spectral photocurrent measurements. In addition, the morphology is manipulated via annealing, to increase the extent of phase separation in the thin-film blends and to identify the distribution of materials. Photoluminescence measurements confirm the demixing of the materials under thermal treatment. Furthermore the photoluminescence of PCBM clusters with sizes of up to a few hundred nanometers indicates a photocurrent loss in films of the coarser phase-separated blends cast from toluene. For toluene-cast films the scale of phase separation depends strongly on the ratio of MDMO-PPV to PCBM, as well as on the total concentration of the casting solution. Finally we observe small beads of 20–30 nm diameter, attributed to MDMO-PPV, in blend films cast from both toluene and chlorobenzene.

1. Introduction

Thin-film organic solar cells based on conjugated polymer/fullerene blends have been subject to increasing interest over the past few years.^[1–5] The main progress in solar-energy conversion efficiency has been achieved by introducing the bulk-heterojunction concept^[6–9] instead of the bilayer structure^[10–16] for the photoactive layer. A similar effect has also been observed for small-molecule solar cells.^[17] The main characteristic

of a bulk heterojunction is the greatly increased interfacial area between the donor and acceptor phases, which enables charge separation within the bulk instead of just at the planar interface of a simple bilayer. The main limiting factors for bilayer devices have been the exciton diffusion length^[13–15] and/or the thickness of a space-charge layer,^[16] both of which have ranges of a few nanometers. Only excitons that are generated within this distance of the bilayer heterojunction interface can contribute to the photogenerated current. In contrast, the bulk-heterojunction device makes use of photon absorption throughout the bulk in the intermixed layer. This has also been shown by optical absorption and photocurrent simulation for the respective device concepts.^[13–16,18]

Recently it was demonstrated that the solvent from which the blend film is cast influences the solar power conversion efficiency dramatically. Upon replacing toluene with chlorobenzene, a more than twofold increase was reported for MDMO-PPV:PCBM-based bulk heterojunctions (MDMO-PPV: poly[2-methoxy-5-(3,7-dimethyloctyloxy)]-1,4-phenylenevinylene; PCBM: 1-(3-methoxycarbonyl) propyl-1-phenyl [6,6]C₆₁).^[9] Atomic force microscopy (AFM) measurements indicated that a finer phase separation in the chlorobenzene-cast films may account for this. Very recently, a combined transmission electron microscopy (TEM) and AFM study — devoted to the same bulk-heterojunction solar cells — showed, that PCBM-rich domains within the blend form clusters in films spin-cast from either toluene or chlorobenzene solutions.^[19] The authors attributed the larger cluster size of the PCBM-rich domains in films spin-cast from toluene solution to the lower solubility of PCBM within this solvent, as compared to chlorobenzene.

Here we report a high-resolution scanning electron microscopy (SEM) and AFM study with a more detailed imaging of

[*] H. Hoppe, C. Winder, Prof. D. Meissner, Prof. N. S. Sariciftci
Linz Institute for Organic Solar Cells (LIOS)

Johannes Kepler University
Altenbergerstr. 69, A-4040 Linz (Austria)
E-mail: harald.hoppe@jku.at

M. Niggemann, Dr. A. Hinsch
Fraunhofer Institute for Solar Energy Systems (ISE)
Heidenhofstr. 2, D-79110 Freiburg (Germany)

Dr. J. Kraut, Prof. R. Hiesgen
University of Applied Sciences
Kanalstraße 33, D-73728 Esslingen (Germany)

C. Winder, Prof. N. S. Sariciftci
Christian Doppler Laboratory for Plastic Solar Cells
Johannes Kepler University
A-4040 Linz (Austria)

Prof. D. Meissner
University of Applied Sciences
Roseggerstr. 12
A-4600 Wels (Austria)

[**] Financial support was provided by the German Ministry for Education and Research (BMBF, contract numbers 01SF0026 and 01SF0119) as well as by an EC INTAS grant (INTAS 00506). Part of this work was performed within the Christian Doppler Society's dedicated laboratory on Plastic Solar Cells. RH and JK thank Berthold Völkel, Institute of Physical Chemistry, University of Heidelberg (Prof. M. Grunze), for the possibility to use their SEM.

the underlying nanomorphology in bulk heterojunctions; we are even able to see polymeric nanospheres of radius ~ 10 nm. Furthermore, we find the larger PCBM clusters to show some residual photoluminescence (PL), thus indicating a specific loss mechanism for photocurrent generation in toluene-cast blends. This is in agreement with results obtained from corresponding solar-cell characterizations. In addition to varying the blending ratios of MDMO-PPV and PCBM, we also vary the total concentration of the casting solution whilst keeping the mixing (blending) ratio constant. Finally, combined AFM and PL measurements on annealed samples lead to the clear identification of the nanospheres as MDMO-PPV, while PCBM reorganizes from the clusters into larger aggregates.

2. Results

In Figure 1 AFM results obtained for films of MDMO-PPV/PCBM 1:4 (by weight) spin-cast from chlorobenzene and from toluene solution are shown. Note that the height-variation profile increases from 10 nm for chlorobenzene- up to more than 100 nm for toluene-cast films. In the case of toluene-cast films the average grain reaches a width of a few hundred nanometers (compare with Fig. 1 in work by Martens et al.^[19]). As shown below, these grains are PCBM clusters, and their size strongly depends on the ratio of PCBM to MDMO-PPV.

2.1. Toluene-Cast Films

A series of films cast from toluene solutions containing different weight ratios of polymer to fullerene was studied using SEM and AFM. The MDMO-PPV concentration in the solution was kept constant at 0.33 wt.-%. In Figure 2 the top views of toluene-cast films of mixing ratio 1:1, 1:2, 1:3, and 1:4 polymer/fullerene (by weight) are shown. With decreasing PCBM content, the nanoclusters become smaller until they are no

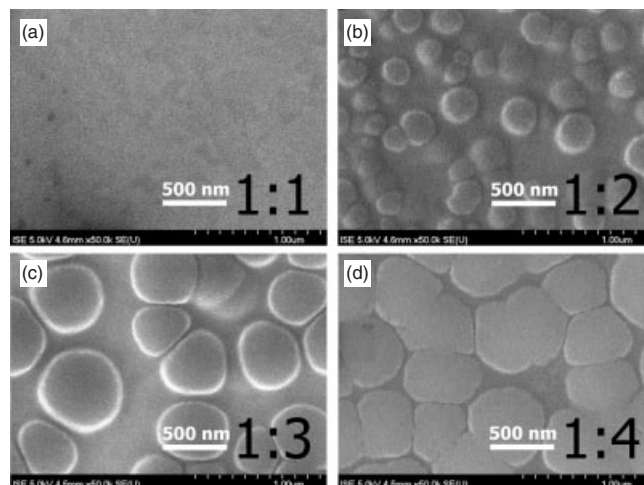


Figure 2. Top views of films cast from toluene with various weight ratios of MDMO-PPV to PCBM measured using SEM. The magnification chosen is 50 000 for all the images. The surface of the 1:1 film (a) looks flat and shows no features. For the films containing a larger percentage of PCBM (b–d), round domains or nanoclusters are visible, increasing in size with increasing PCBM content. Due to the high PCBM content in the film with a 1:4 ratio (d), the clusters come into close proximity and lose their round shape.

longer be observed, as is the case for the 1:1 films. Martens et al.^[19] claim the existence of a homogeneous blend for the 1:1 toluene-based mixture, as single PCBM clusters in the film cannot be detected using transmission electron microscopy (TEM). To gain insight into the nanostructure within the films, the samples were broken and then the cross-sections were imaged using SEM. Figure 3 shows cross-sections of the films presented in Figure 2. Here it can be clearly seen that in heavily PCBM-loaded films the PCBM nanoclusters are generally covered by another “skin” layer of thickness approximately 20–40 nm. The shape of these nanoclusters is somewhat flattened, i.e., somewhat disk-like, as their radius exceeds the film

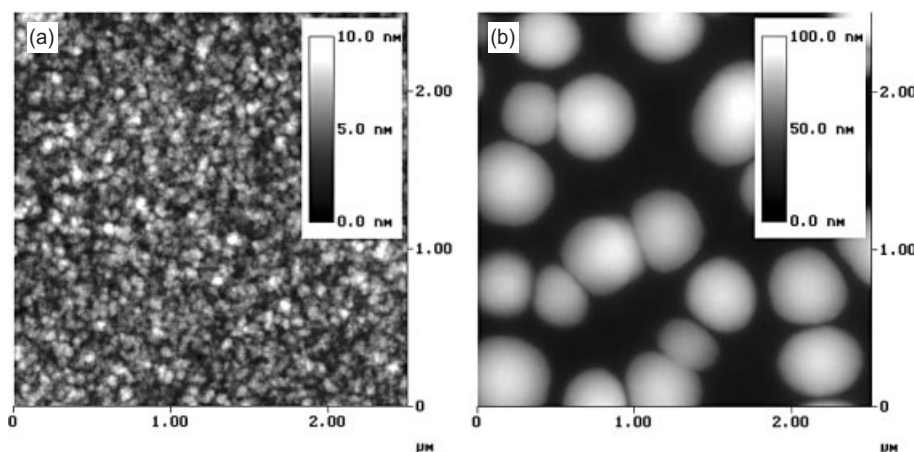


Figure 1. AFM topography scans of MDMO-PPV/PCBM 1:4 (by weight) blended films spin-cast from a) chlorobenzene (1.4 wt.-%) and b) toluene solution (1 wt.-%). The toluene-cast film shows a tenfold greater height variation as compared to the chlorobenzene-cast one. Features of a few hundred nanometers in width are visible in (b), while features in (a) are around 50 nm. The scan size is 2.5 μ m in both cases.

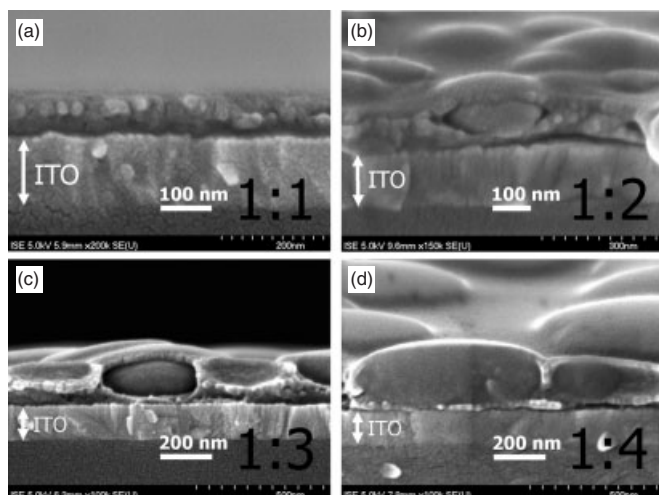


Figure 3. SEM side views (cross-sections) of MDMO-PPV/PCBM blend films cast from toluene with various weight ratios of MDMO-PPV and PCBM. For the ratios 1:4, 1:3, and 1:2 (b–d) the nanoclusters, in the form of discs, are surrounded by another phase, called the skin, that contains smaller spheres of about 20–30 nm diameter. For the 1:1 film, only these smaller spheres are found. The magnifications used are 100 000 (c,d), 150 000 (b), and 200 000 (a).

thickness. For the 1:1 blend, small nanospheres are embedded within a rather homogeneous matrix. Their diameter (about 20–30 nm) is much smaller than the film thickness and hence they are not apparent in the top-view scans. These nanospheres are also found around the larger nanoclusters within the skin layer.

In Figure 4 samples spin-cast and drop-cast from toluene solution are compared. Larger and coalesced structures are found in the case of the drop-cast samples (Fig. 4b). Recently it was demonstrated that the solvent-evaporation time has an influence on the resulting morphology of a solution-cast film, even when all other parameters such as solution concentration and film thickness are kept constant.^[20] There, slower solvent evaporation yielded a coarser phase separation, which is in agreement with our observations.

Solutions of different concentrations, but with constant component ratios of 1:4 MDMO-PPV/PCBM have been prepared. In this case, the total polymer and fullerene content in the solu-

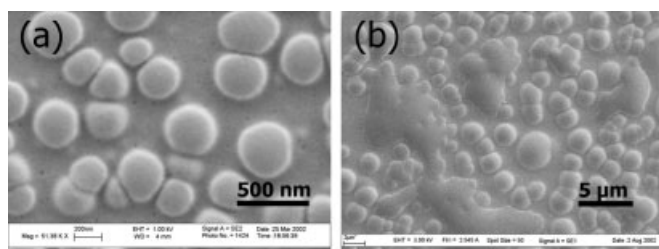


Figure 4. SEM comparison between a spin-cast (a) (MDMO-PPV/PCBM 1:3, 1 wt.-% in solution) and a drop-cast (b) (1:4, 1.5 wt.-% in solution) film of in toluene solution. The clusters in the spin-cast film do not coalesce, whilst for the drop-cast film, extended coalescence is noticed. Note that the magnification of (a) is about one order of magnitude larger than that of (b).

tions ranges from 0.50 up to 1.50 wt.-%, which corresponds to 0.10 to 0.30 wt.-% concentrations of MDMO-PPV in the solution. AFM scans reveal that the fullerene cluster size (Fig. 5), as well as the average film thickness, increases on increasing total concentration.

2.2. Chlorobenzene-Cast Films

In Figure 6, side-view cross-sections of the chlorobenzene-cast films are shown for mixing ratios of 1:2, 1:4, and 1:6 MDMO-PPV/PCBM. All of these films appear to be homogeneous except for some smaller nanospheres (around 20 nm in diameter), which are dispersed throughout the films. The size of these nanospheres does not change with PCBM content, but is comparable with the nanospheres observed in the toluene-cast composite films. The size of any possible clusters of PCBM must be much smaller than for the toluene-cast films. However, for the 1:6 blend, larger clusters can be seen. These are surrounded by nanospheres — as in the case of toluene-cast films — in a “skin” layer. Interestingly, a preferential adsorption of the nanospheres on top of the PEDOT:PSS (poly(3,4-ethylenedioxy thiophene):poly(styrene sulfonate)) anode layer is also found.

2.3. Annealing of Blended Films from Both Solvents

Thin films spin-cast from 0.50 wt.-% (total concentration of polymer and PCBM) toluene solutions and 1.40 wt.-% (total concentration, again) chlorobenzene solutions have been comparatively studied by annealing at temperatures around 145 (±5) °C. In Figure 7, AFM images of samples annealed for different times, ranging from several minutes to a few hours, are depicted for toluene- and chlorobenzene-based films. As a result of the annealing process, the PCBM phase forms evolving microstructures, i.e., crystalline aggregates.^[21] The different stages in annealing of the toluene-based films reveal how the crystallites are formed. First, after a few minutes, the whole film shows some surface roughening, which results in “blurring” of the AFM image, compared to the scan in Figure 1b. This may correspond to some local reorganization of the polymer-rich phase or some release of therein-embedded PCBM. Next, small crystallites are formed and grow at the expense of the surrounding rounding clusters (Fig. 7a). After 30 min the crystallites are continuously growing at the expense of the closest PCBM nanoclusters (Fig. 7b). Finally, after roughly 4 h (Fig. 7c), most of the round PCBM nanoclusters have disappeared, leaving some circular holes behind (Fig. 7d). The continuous matrix framework around these holes consists of small nanospheres of about 30–40 nm, which is comparable to the results of the SEM measurements obtained for cross-sections of the toluene-cast films, if a finite radius of curvature (5–10 nm) for the AFM tip is taken into account. As the annealing has caused most of the PCBM to diffuse and organize into crystallites, it is reasonable to identify these nanospheres as polymeric nanostructures.

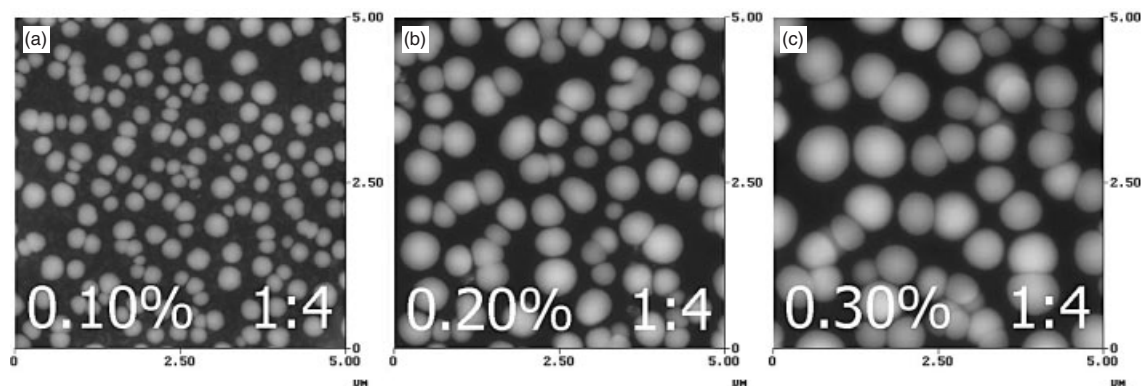


Figure 5. AFM scans of films spin-cast from toluene with the same ratio of MDMO-PPV to PCBM (1:4 by weight), but with different total concentrations in the precursor toluene solution. Increasing the total concentration from 0.50 wt.-% up to 1.50 wt.-% (MDMO-PPV concentration, 0.10 wt.-% and 0.30 wt.-%, respectively) results in a strong increase of the PCBM cluster sizes. Scan sizes are in all cases $5 \mu\text{m} \times 5 \mu\text{m}$; z-ranges are 100 nm (a), 150 nm (b), and 200 nm (c).

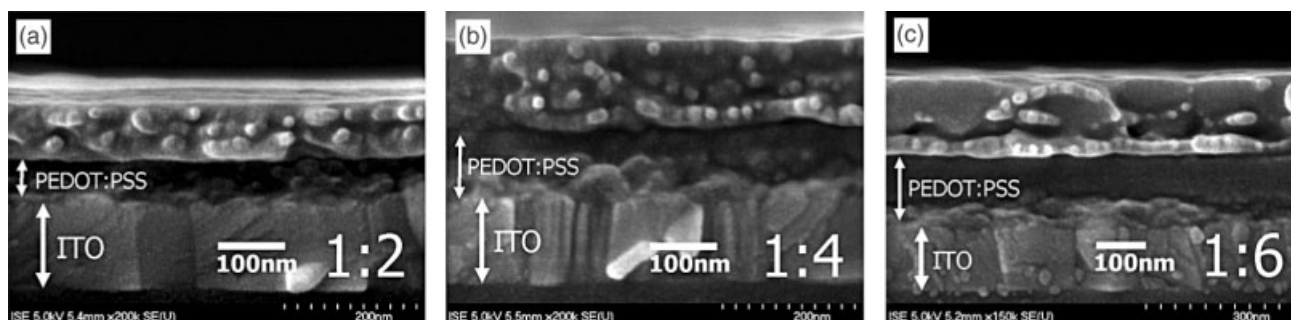


Figure 6. SEM side views (cross-sections) of MDMO-PPV:PCBM blend films spin-cast from chlorobenzene solutions with various ratios (by weight) of MDMO-PPV to PCBM on top of PEDOT:PSS-coated ITO glass. In all samples nanospheres of about the same size (20 nm) are found. The magnifications used are 200 000 (a,b) and 150 000 (c).

The same annealing was performed for about 30 min on a film cast from chlorobenzene solution (compare Figs. 7e,f). The crystallites that evolved here seem to be smoother, which indicates a more homogenous growth process. Between these crystallites, the originally flat film was still present (as seen in the higher-magnification image, Fig. 7f), and it is only in close proximity to the crystallites that the film morphology had been altered considerably as a result of the depletion of the PCBM phase.

2.4. Photoluminescence

Room-temperature PL spectra of films of pristine MDMO-PPV, PCBM, and blends (1:4) of the two have been obtained using an argon-ion laser at 476 nm as an excitation light source (see Fig. 8). After annealing, the spectral shape of the PL of MDMO-PPV changes slightly. This is ascribed to ordering taking effect during annealing at temperatures higher than the glass-transition temperature of MDMO-PPV. Compared to the polymer, the PCBM film showed a much weaker PL, which is mainly attributed to a less efficient emission resulting from

symmetry-forbidden singlet radiative recombination as well as efficient intersystem crossing to the triplet state.^[22] For the chlorobenzene-cast blend film there is no luminescence detectable, which indicates complete exciton dissociation at the polymer–fullerene bulk interface. In contrast, the corresponding films spin-cast from toluene solution show some photoluminescence of PCBM. We attribute this to the radiative recombination of excitons within the quite large PCBM nanoclusters, before they can reach the phase interface. Thus for increasing PCBM cluster sizes (compare Figs. 5,8), the PL signal of PCBM likewise increased. In addition, the observation of the PL indicates the PCBM nanoclusters to be rather pure, since charge transfer to possibly embedded MDMO-PPV would otherwise quench this PL. Upon annealing of the blend films, the MDMO-PPV PL is again apparent, as a result of the depletion of the PCBM phase within the polymer matrix upon crystallization of the PCBM. Because of the strong polymer PL, the PL signal of the PCBM could no longer be distinguished after annealing. Therefore, we selectively excited the PCBM using a 664 nm diode laser. At this wavelength the polymer is almost non-absorbing and we clearly detected the PL of PCBM from the annealed film.

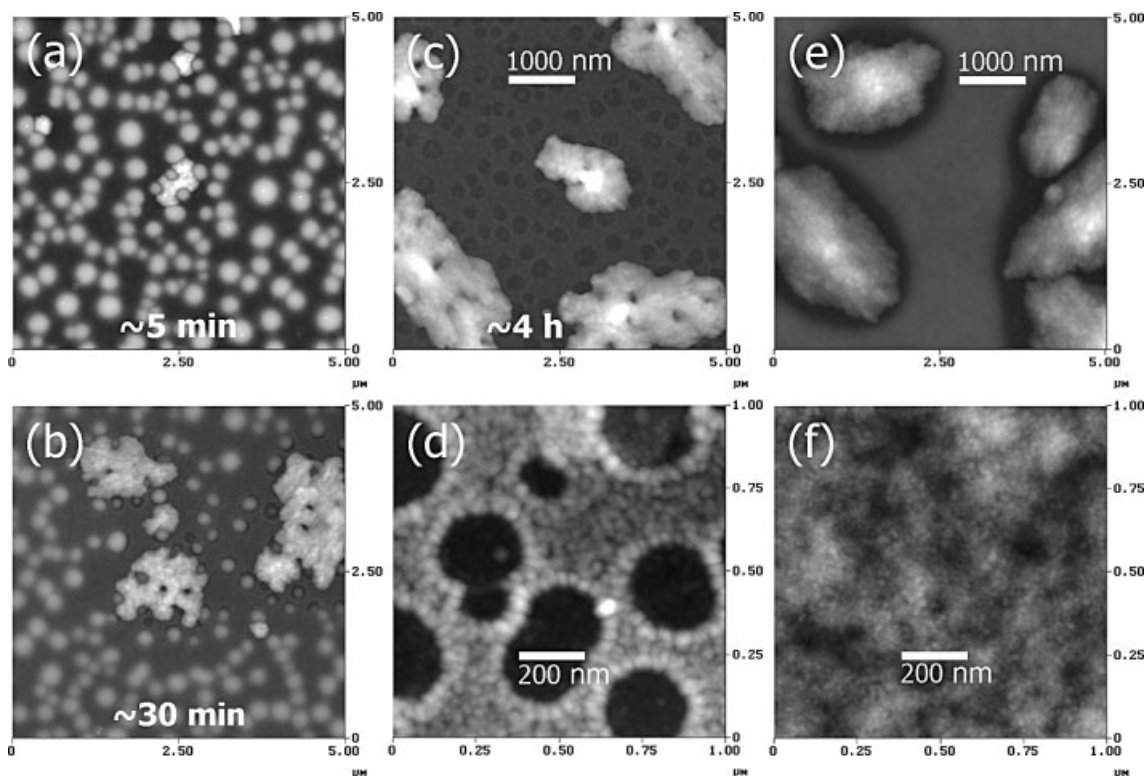


Figure 7. AFM topography of annealed films of MDMO-PPV:PCBM spin-cast from toluene (a–d) (0.50 wt.-%, 1:4 MDMO-PPV/PCBM) and chlorobenzene (e,f) (1.40 wt.-% 1:4 MDMO-PPV/PCBM). For increased annealing times (a–c), larger and larger crystals are formed at the expense of surrounding PCBM clusters. At high magnification (d), at the end of the annealing process, holes are evident where there have previously been PCBM clusters. For the films spin-cast from chlorobenzene (e,f), similar crystals appear, but they seem to grow more homogeneously in comparison with those in films cast from toluene. In addition, the process in (e) is not completed, as in (f) (magnification of (e)) the originally flat film topography between the large crystallites is quite preserved. In (d), the framework consists of about 30–40 nm diameter spheres in close agreement with the nanospheres found in the SEM images of the cross-sections. Scan sizes are $1\ \mu\text{m} \times 1\ \mu\text{m}$ for (d,f) and $5\ \mu\text{m} \times 5\ \mu\text{m}$ for (a–c,e). Z-ranges are 100 nm, 200 nm, 300 nm, 25 nm, 300 nm, and 15 nm for (a–f), respectively.

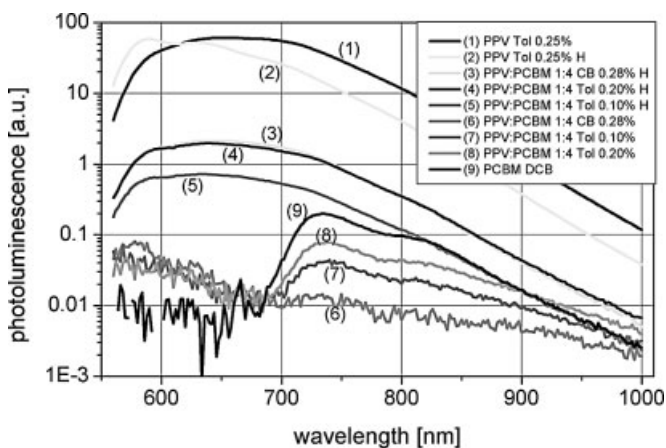


Figure 8. PL spectra of films of pristine MDMO-PPV (peak between 580 and 700 nm), pristine PCBM (peak at ~ 735 nm), and MDMO-PPV/PCBM blends (1:4) of films cast from either toluene or chlorobenzene solution. While the unannealed blend film from chlorobenzene shows no detectable luminescence, the blends spin-cast from toluene clearly display luminescence from PCBM. This is attributed to the radiative recombination of excitons within the PCBM nanoclusters that do not reach the interface with the MDMO-PPV-rich phase. The labels specify the material, the solvent (Tol = toluene, CB = chlorobenzene, DCB = dichlorobenzene), the polymer concentration, and whether the film was heated (noted with H).

2.5. Solar-Cell Devices

Bulk-heterojunction solar cells were prepared with different weight ratios of MDMO-PPV to PCBM, and using different solvents, toluene and chlorobenzene, as discussed above. The devices were characterized by current–voltage (I – V) and spectral photocurrent measurements. The results for the basic device parameters at $80\ \text{mW cm}^{-2}$ white light from a solar simulator are shown in Table 1 (films cast from toluene) and Table 2 (films cast from chlorobenzene). In the case of toluene-cast films, we find generally lower photocurrents (I_{SC} , short-circuit current), resulting in lower power conversion efficiencies (η) as compared with chlorobenzene-cast devices. On the other hand, the open-circuit voltages (V_{OC}) and the fill factors (FF) are of comparable magnitude. For toluene-cast films, upon increasing the PCBM concentration, we find the photocurrent to become saturated. This may be a result of an increasing inactive volume inside the relatively large PCBM domains which does not affect the photocurrent generation at the phase boundary. Also, in chlorobenzene-cast films, when the PCBM concentration is increased beyond an optimum value, some photocurrent is lost. This may be a result of a decrease in the interfacial area and corresponding loss of percolation opportunity for

Table 1. Device parameters for toluene-cast active layers. Solutions are of different PCBM content but of equal polymer concentration (0.33 wt.-%).

MDMO-PPV/PCBM ratio [wt.]	Short-circuit current, I_{SC} [mA m ⁻²]	Fill factor, FF	Open-circuit voltage, V_{OC} [V]	Power conversion efficiency, η [%]
1:1	0.93	0.36	0.87	0.36
1:2	1.46	0.46	0.84	0.68
1:3	1.49	0.48	0.82	0.72
1:4	1.49	0.49	0.82	0.74

Table 2. Device parameters for chlorobenzene-cast active layers. Solutions are of different PCBM content but of equal polymer concentration (0.35 wt.-%).

MDMO-PPV/PCBM ratio [wt.]	Short-circuit current, I_{SC} [mA m ⁻²]	Fill factor, FF	Open-circuit voltage, V_{OC} [V]	Power conversion efficiency, η [%]
1:2	1.89	0.44	0.85	0.86
1:4	3.03	0.5	0.84	1.59
1:6	2.54	0.36	0.78	0.89

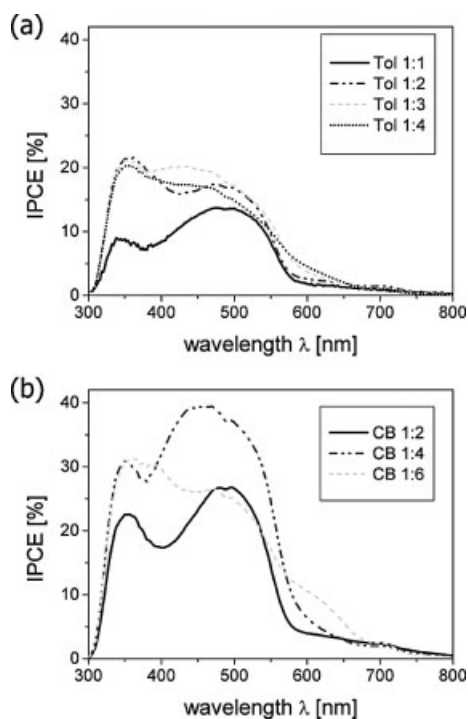


Figure 9. Spectral photocurrent (IPCE: incident-photon-to-collected-electron (ratio)) of solar-cell devices with active layers of different ratios of MDMO-PPV/PCBM cast from a) toluene (compare with Figs. 2,3) and b) chlorobenzene (compare with Fig. 6).

hole transport through the bulk of the active layer (compare with Fig. 6, 1:6). The results from spectral photocurrent measurements are shown in Figure 9. They reconfirm, that the currents from chlorobenzene-cast films are generally higher than those from toluene-cast films. In addition the signature of the

PCBM absorption (compare with previous results^[18]) becomes more visible for increased PCBM content between 600 and 650 nm.

3. Discussion

The more efficient bulk-heterojunctions spin-cast from chlorobenzene precursor solutions show a finer phase distribution than those cast from toluene solutions. In the latter we observed quenched PL from PCBM, indicating the existence of pure PCBM domains that are considerably larger than the exciton diffusion range. This is in agreement with the observation of large nanoclusters, which increase in size with higher PCBM loading, in toluene-cast blends. These nanoclusters are presumed to limit charge generation as their formation leads to a reduced interfacial area between the PCBM and the MDMO-PPV-rich phase. Such aspects of nanostructure are therefore critical for the efficiency of solar cell.

During annealing of toluene-cast blend films, the diffusion of PCBM molecules, from the nanoclusters into larger crystallites, leads to the formation of holes. AFM analysis showed that small beads exist around these holes, reminiscent of the nanospheres detected in unannealed films using SEM. From the PL measurements we conclude that the annealing leads to a coarse phase separation of MDMO-PPV and PCBM. This phase separation cannot be complete, as the luminescence is still 1–2 orders of magnitude lower than that obtained from pristine MDMO-PPV. The recurrence of the PL signal from MDMO-PPV confirms that the nanospheres found in the skins around the PCBM nanoclusters in the toluene-cast films and distributed in films from both solvents, may represent the polymer. Polymers self-organize into a coiled structure in solution^[23] and such behavior is consistent with the formation of the nanospheres. The size of the nanospheres is comparable with the hydrodynamic radii obtained from light scattering on chlorobenzene and *p*-xylene solutions of a very similar PPV derivative.^[24–25]

In summary, the large clusters are assigned to the bare PCBM phase, while the small nanospheres are assigned to the polymer.

4. Conclusions

The nanoscale morphology within the photoactive blends of conjugated polymers and fullerenes has been investigated by means of SEM and AFM. In combination with annealing studies and PL measurements, the distribution of fullerene and polymer domains in the solution-cast films has been identified. Moreover solar-cell characteristics have been connected to the observed morphology. Such an understanding of the relationship between the nanoscale morphology and the photovoltaic properties of blend films cast from solution can be used for the future optimization of bulk-heterojunction plastic solar cells.

5. Experimental

General: All films were prepared under ambient conditions. PEDOT:PSS was spin-cast from an aqueous solution of concentration 0.5 wt.-%. The photoactive films were prepared by spin- or drop-casting from either toluene or chlorobenzene solutions of the blended materials onto glass, indium tin oxide (ITO)-coated, or ITO-glass/PEDOT:PSS substrates. The spin-casting procedure involved 40 s of spinning at 1500 rpm followed by 20 s at 2000 rpm. The single-drop-cast film (shown in Fig. 4b) was prepared under N₂ flow at room temperature and dried for 1–2 h. The films were dried in a vacuum chamber (at a few mbar) for about 30 min at room temperature. All solutions were prepared by dissolving the MDMO-PPV and the PCBM directly in the respective solvent. They were stirred overnight under ambient (for chlorobenzene) or slightly elevated (for toluene, 50 °C) temperatures, with neither sonication nor filtering. AFM measurements were performed with a Dimension 3100 system (Digital Instruments, Santa Barbara, CA) operating in tapping mode. SEM measurements were performed using a Cold-Field-Emission Scanning Electron Microscope Hitachi S-4700. Prior to imaging, the samples were covered by a thin sputtered layer of platinum on either their broken edge or on their upper surface. The SEM measurements in Figure 4 were performed using a) a LEO Gemini 1530 and b) LEO 1455 VP (LEO GmbH, Oberkochen, Germany) instruments with no sputtered layer coating the samples.

The PL of thin films on glass was measured at room temperature under a dynamic vacuum ($p < 10^{-5}$ mbar). The PL signal was dispersed using a grating with an additional set of filters. The signal was recorded using a Si detector and a lock-in amplifier. The spectra are corrected for the set-up response. The samples were excited with an Ar⁺ laser operating at 476 nm and 40 mW on a spot size of diameter 4 mm. The beam was chopped with a frequency of 41 Hz. To evaluate PCBM PL in the annealed samples, a diode laser operating at 664 nm was used for selective excitation. The laser beam was blocked at the detector using a high-pass filter of 695 nm.

Solar-cell devices were prepared in thin-film geometry. A layer of PEDOT:PSS and the active layer were spin-cast on a substrate of pre-cleaned ITO. For the top electrode, LiF (6 Å) and Al (80 nm) were evaporated under vacuum at 10⁻⁵ mbar. Characterization of the devices was carried out under an argon atmosphere. *I*-*V* measurements were performed using a solar simulator (Steuernagel 575) operating at 80 mW cm⁻² to simulate AM1.5 solar irradiation. The spectral photocurrent was recorded under illumination by a monochromatized xenon lamp with a typical illumination density of 5–10 μW. The incident beam was chopped with a mechanical chopper, the photocurrent was detected with a lock-in-amplifier. The Xe-lamp spectrum was measured with a calibrated Si diode.

Materials: MDMO-PPV (poly[2-methoxy-5-(3,7-dimethyloctyloxy)]-1,4-phenylenevinylene) with a molecular weight of about 10⁶ (weight-average molecular weight, $M_w = 1\,150\,000$ g mol⁻¹; number-average molecular weight, $M_n = 170\,000$ g mol⁻¹), and a glass-transition temperature of about 65 °C was provided by Covion (Germany) [26]. PCBM (1-(3-methoxycarbonyl) propyl-1-phenyl [6,6]C₆₀) of purity better than 99.5 % was purchased from J. C. Hummelen (Univ. of Groningen, The Netherlands). PEDOT:PSS (poly(3,4-ethylenedioxy thiophene):poly(styrene sulfonate)) (Baytron P) was purchased from Bayer (Germany). ITO-coated glass was purchased from Merck (Germany).

Received: September 3, 2003

Final version: April 19, 2004

- [1] C. J. Brabec, N. S. Sariciftci, J. C. Hummelen, *Adv. Funct. Mater.* **2001**, *11*, 15.
- [2] V. Dyakonov, *Phys. E (Amsterdam, Neth.)* **2002**, *14*, 53.
- [3] *Organic Photovoltaics* (Eds: C. J. Brabec, V. Dyakonov, J. Parisi, N. S. Sariciftci), Springer Series in Materials Science, Vol. 60, Springer, Berlin, Germany **2003**.
- [4] J. Nelson, *Curr. Opin. Solid State Mater. Sci.* **2002**, *6*, 87.
- [5] J.-M. Nunzi, *C. R. Phys.* **2002**, *3*, 523.
- [6] G. Yu, A. J. Heeger, *J. Appl. Phys.* **1995**, *78*, 4510.
- [7] G. Yu, J. Gao, J. C. Hummelen, F. Wudl, A. J. Heeger, *Science* **1995**, *270*, 1789.
- [8] J. J. M. Halls, C. A. Walsh, N. C. Greenham, E. A. Marseglia, R. H. Friend, S. C. Moratti, A. B. Holmes, *Nature* **1995**, *376*, 498.
- [9] S. E. Shaheen, C. J. Brabec, N. S. Sariciftci, F. Padinger, T. Fromherz, J. C. Hummelen, *Appl. Phys. Lett.* **2001**, *78*, 841.
- [10] C. W. Tang, *Appl. Phys. Lett.* **1986**, *48*, 183.
- [11] D. Wöhrle, D. Meissner, *Adv. Mater.* **1991**, *3*, 129.
- [12] N. S. Sariciftci, D. Braun, C. Zhang, V. I. Srdanov, A. J. Heeger, G. Stucky, F. Wudl, *Appl. Phys. Lett.* **1993**, *62*, 585.
- [13] J. J. M. Halls, K. Pichler, R. H. Friend, S. C. Moratti, A. B. Holmes, *Appl. Phys. Lett.* **1996**, *68*, 3120.
- [14] a) L. S. Roman, W. Mammo, L. A. A. Pettersson, M. R. Andersson, O. Inganäs, *Adv. Mater.* **1998**, *10*, 774. b) L. A. A. Pettersson, L. S. Roman, O. Inganäs, *J. Appl. Phys.* **1999**, *86*, 487.
- [15] T. Stübinger, W. Brütting, *J. Appl. Phys.* **2001**, *90*, 3632.
- [16] a) P. A. Lane, J. Rostalski, C. Giebeler, S. J. Martin, D. D. C. Bradley, D. Meissner, *Sol. Energy Mater. Sol. Cells* **2000**, *63*, 3. b) J. Rostalski, D. Meissner, *Sol. Energy Mater. Sol. Cells* **2000**, *63*, 37. c) J. Rostalski, D. Meissner, *Synth. Met.* **2001**, *121*, 1551.
- [17] M. Hiramoto, H. Fujiwara, M. Yokoyama, *J. Appl. Phys.* **1992**, *8*, 3781.
- [18] H. Hoppe, N. Arnold, N. S. Sariciftci, D. Meissner, *Sol. Energy Mater. Sol. Cells* **2003**, *80*, 105.
- [19] T. Martens, J. D'Haen, T. Munters, Z. Beelen, L. Goris, J. Manca, M. D'Olieslaeger, D. Vanderzande, L. De Schepper, R. Andriessen, *Synth. Met.* **2003**, *138*, 243.
- [20] T. Martens, Z. Beelen, J. D'Haen, T. Munters, L. Goris, J. Manca, M. D'Olieslaeger, D. Vanderzande, L. De Schepper, R. Andriessen, *Proc. SPIE-Int. Soc. Opt. Eng.* **2002**, *4801*, 40.
- [21] Transmission electron microscopy shows a diffraction pattern of hexagonal reflections due to the crystalline structure of the aggregates.
- [22] M. S. Dresselhaus, G. Dresselhaus, P. C. Eklund, *Science of Fullerenes and Carbon Nanotubes*, Academic Press, San Diego, CA **1996**, Ch. 13.
- [23] a) P. J. Flory, *Principles of Polymer Chemistry*, Cornell University Press, Ithaca, NY **1953**. b) P. G. de Gennes, *Scaling Concepts in Polymer Physics*, Cornell University Press, Ithaca, NY **1979**. c) M. Doi, *Introduction to Polymer Physics*, Clarendon Press, Oxford, UK **1996**.
- [24] C. L. Gettenger, A. J. Heeger, J. M. Drake, D. J. Pine, *J. Chem. Phys.* **1994**, *101*, 1673.
- [25] T. Q. Nguyen, V. Doan, B. J. Schwartz, *J. Chem. Phys.* **1999**, *110*, 4068.
- [26] H. Becker, Covion Organic Semiconductors GmbH, Frankfurt, Germany, personal communication.